12WCEE 2000

0263

FINITE ELEMENT TECHNIQUES FOR SIMULATION OF INFILLED REINFORCED CONCRETE BUILDINGS UNDER EARTHQUAKE LOADING

Flavio M B GALANTI[1], Tom SCARPAS[2] And Anton C W VROUWENVELDER[3]

SUMMARY

An alternative approach is presented for the solution of non-linear structural problems typically encountered in the field of earthquake engineering. The proposed methodology makes use of an indirect solution method and avoids the computation of stiffness matrices. Consequently, the difficulties normally related to the use of stiffness matrices in the classical solution methods are eliminated. The approach allows for treatment of both static and dynamic problems. Examples are presented for the case of a reinforced concrete frame with and without infill modelled using finite elements, demonstrating the effectiveness of the approach in the analysis of non-linear structural problems.

INTRODUCTION

The non-linear finite element analysis of structures made from brittle materials such as masonry and concrete is often made difficult due to the inherent unstable response of such materials. The formation of cracks in these materials can lead to substantial changes in the distribution of forces and sudden reductions in structural resistance, which can severely affect the performance of the algorithms used for solving the equations of equilibrium. In terms of the numerical process, this implies the introduction of very small or zero stiffness terms in the global stiffness matrix making its inversion less accurate and introducing large differences between each iteration of the solution process. The result is that the solution process at some stage of the analysis persistently does not converge and at times even diverges. In the past, the authors have analysed masonry walls and infilled r.c. frames subject to monotonically increasing static loads [Galanti, Scarpas and Vrouwenvelder, 1998a, b] and have encountered systematically these types of problems. The obtained results were mostly limited to the initial response of the analysed structures and their potential load bearing capacity. For the earthquake engineer this unreliability of the numerical tools is rather restrictive, since normally one wishes to obtain information as to the ductility and energy dissipation characteristics of a particular structure.

AN ALTERNATIVE APPROACH FOR THE NON-LINEAR FINITE ELEMENT ANALYSIS OF STRUCTURES

A way to try to improve the convergence of the solution process is to resort to a dynamic analysis rather than a static analysis. Although the results of the two types of analyses will clearly be different, if the problems of numerical instability are caused by singularities in the computed stiffness matrices or due to an ill-conditioning thereof, then the inclusion of inertial effects may result in an improved numerical performance with respect to the static analysis. Denoting **M** as the mass matrix of the system, **a** as the vector of nodal accelerations, **R** as the vector of internal forces and **P** as the applied external load, we can write the semi-discrete equation of motion for a system with *n* degrees of freedom as follows:

$$\mathbf{Ma} + \mathbf{R} = \mathbf{P} \tag{1}$$

Introducing any given integration scheme (for instance Newmark's method) the problem of finding the future response of the system at the end of a step is reduced to that of solving a system of non-linear equations, which normally is carried out using the Newton method. Nonetheless, problems may persist due to the necessity of

[1] *Faculty of Civil Eng and Geosciences, Delft Uni of Technology, Stevinweg, Netherlands e-mail: F.Galanti@CT.TUDelft.NL*
[2] *Faculty of Civil Eng and Geosciences, Delft University of Technology, Stevinweg, The Netherlands*
[3] *Faculty of Civil Eng and Geosciences, Delft University of Technology, Stevinweg, The Netherlands*

computing the stiffness matrix, and this may require the use of smaller time steps in the analysis, making the total computation time increase. This, and the possibility of not converging, has led the authors to implement a method for the dynamic analysis of structures which does not require the use of stiffness matrices [Galanti, Scarpas and Vrouwenvelder, to be publ.]. Further, a scheme will be introduced, which by retaining the dynamic nature of the problem, finds an approximation of the static solution for a given load level.

An indirect solution method for the dynamic problem

The use of the stiffness matrix can be avoided by resorting to the method discussed here, which even though not of an explicit nature, does not require the use of these matrices. The method will be given for the particular case where the integration of the equations of motions is carried out using the trapezoidal method, (i.e. Newmark's method with γ=0.5 and β=0.25), in which the velocities, $\mathbf{v}_1$, and displacements, $\mathbf{u}_1$, of the system at the end of a step are given by:

$$\begin{aligned}\mathbf{v}_1 &= \mathbf{v}_0 + \Delta t\left(\dot{\mathbf{v}}_0 + \dot{\mathbf{v}}_1\right)/2 \\ \mathbf{u}_1 &= \mathbf{u}_0 + \Delta t\left(\dot{\mathbf{u}}_0 + \dot{\mathbf{u}}_1\right)/2\end{aligned} \tag{2}$$

where the indices 0 and 1 refer to the values of the variables at the start and end of the step, respectively. Substituting the accelerations using the equation of motion 1, and rewriting 2 expressing the variations in the velocities, $\Delta\mathbf{v}$, and displacements, $\Delta\mathbf{u}$, the following expressions are obtained:

$$\begin{aligned}\Delta\mathbf{v} &= \Delta t\mathbf{M}^{-1}\left(\mathbf{P}_0 - \mathbf{R}_0 + \mathbf{P}_1 - \mathbf{R}_1\right)/2 \\ \Delta\mathbf{u} &= \Delta t\left(\mathbf{v}_0 + \Delta\mathbf{v}/2\right)\end{aligned} \tag{3}$$

where $\Delta\mathbf{v}$= $\mathbf{v}_1$- $\mathbf{v}_0$; and $\Delta\mathbf{u}$= $\mathbf{u}_1$- $\mathbf{u}_0$. The following algorithm is then used:

$$\begin{aligned}\Delta\mathbf{v}^{(1)} &= \Delta t\mathbf{M}^{-1}\left[\left(\mathbf{P}_0 + \mathbf{P}_1\right)/2 - \mathbf{R}_0\right] \\ \Delta\mathbf{u}^{(1)} &= \Delta t\left(\mathbf{v}_0 + \Delta\mathbf{v}^{(1)}/2\right)\end{aligned} \tag{4}$$

$$\begin{aligned}\delta\mathbf{v}^{(i+1)} &= \Delta t\mathbf{M}^{-1}\left(\mathbf{R}_1^{(i-1)} - \mathbf{R}_1^{(i)}\right)/2 \\ \delta\mathbf{u}^{(i+1)} &= \Delta t\delta\mathbf{v}^{(1)}/2\end{aligned} \tag{5}$$

where the index in brackets refers to the iteration number; $\delta\mathbf{v}$ and $\delta\mathbf{u}$ indicate the variations in the displacements and velocities from one iteration to another. It can be shown that the algorithm converges as long as the following condition is met:

$$\Delta t < \frac{2}{\max\left(\omega_j\right)} \quad j = 1\ldots n \tag{6}$$

where ω_j represents the j^{th} angular frequency of the system. This method, given equal step size, produces results which are identical to those that would be obtained using the Newton method.

Determination of the static response

The lack of stiffness formulation from the above algorithm makes the use of relatively short codes possible as specific solver related subroutines and the appropriate element stiffness subroutines are not necessary. On the other hand, this means static problems cannot be solved directly. However, with the introduction of either material or algorithmic damping and by performing the analysis for a large enough number of steps at a constant load level, it is possible to obtain the static response. The choice of the type of damping should be such so as to allow the determination of the static solution within a certain degree of accuracy in the least number of steps. In the presented analyses an artificial damping is introduced by changing the integration scheme as follows:

$$\begin{aligned}\mathbf{v}_1 &= \mathbf{v}_0 + \Delta t\left(\dot{\mathbf{v}}_0 + \dot{\mathbf{v}}_1\right)/2 \\ \mathbf{u}_1 &= \mathbf{u}_0 + \Delta t\left(\dot{\mathbf{u}}_0 + \dot{\mathbf{u}}_1\right)/2\end{aligned} \quad \rightarrow \quad \begin{aligned}\mathbf{v}_1 &= \varphi\,\mathbf{v}_0 + \Delta t\left(\dot{\mathbf{v}}_0 + \dot{\mathbf{v}}_1\right)/2 \\ \mathbf{u}_1 &= \mathbf{u}_0 + \Delta t\left(\dot{\mathbf{u}}_0 + \dot{\mathbf{u}}_1\right)/2\end{aligned}$$

where ϕ is a function which takes on values between 0 and 1 and depends on the history of the motion of the system and the current values of the state variables. Ideally, as the system approaches a level of minimum potential energy the value of ϕ should be chosen closer to 0 than to 1 so that kinetic energy is removed from the system. In the analysed cases the value of ϕ is taken equal to 1 and the response of the system at the end of the step is determined normally. Then the accelerations of the system at the start of the step are compared with those at the end of the step. If the accelerations have increased the step is recalculated with ϕ=0. As a measure to assess whether the accelerations of the system have increased an acceleration norm, *A*, is defined:

$$A = \sqrt{\mathbf{a} \cdot \mathbf{a}} \tag{7}$$

in which the accelerations of the system are calculated as follows:

$$\mathbf{a} = \mathbf{M}^{-1}\left(\mathbf{F}_{ext} - \mathbf{R}\right) \tag{8}$$

where $\mathbf{F}_{ext}$ is the (constant) load being applied. If the accelerations of the system, in absolute sense, have increased during the step, then the system is departing from the equilibrium position. For example, in a free vibrating single degree of freedom system an increase in the acceleration implies an increase of the displacement as acceleration and displacement are directly proportional to each other. Extending this concept to a multi-degree of freedom system the only way to assess whether the system is anywhere close to equilibrium is to calculate the accelerations, hence the introduction of the norm in equation 7. Thus if the accelerations have increased the step is recalculated with the initial velocities set to zero. In essence kinetic energy is removed from the system when a configuration of minimal acceleration is obtained. Figure 1 shows schematically how this works for a free vibrating single degree of freedom system. The procedure can be stopped once the calculated acceleration norm is lower than a user specified minimum.

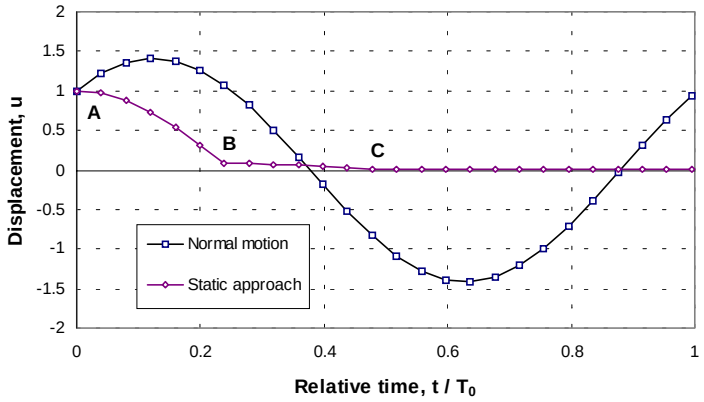

Figure 1. Approach to finding the equilibrium point for a free vibrating single degree of freedom system. At the points A, B and C, the kinetic energy of the system has been removed (the initial velocity for the respective steps is simply set to zero). This is based on the fact that under normal circumstances, the acceleration (and displacement) of the system at the end of the respective steps would have increased.

Displacement controlled analysis

The fact that the load bearing capacity of a structure is not known a-priori implies the application of displacement control in the analysis. To extend the idea of displacement control to dynamic analyses it is only necessary to specify time-displacement diagrams for specific nodes. At specific displacement levels where the static structural response is required the 'static' approach described above will be applied.

MATERIAL RESPONSE MODELLING OF MASONRY AND CONCRETE

In the analyses concrete and masonry are modelled using the same type of element (an 8 noded plane stress quadrilateral element with 3 by 3 integration points) and same material model.

A rotating elastic damage model for concrete and masonry

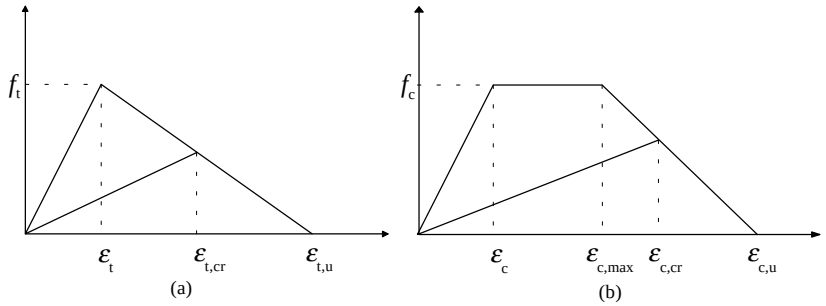

Figure 2. Material response: (a) in tension; (b) in compression.

The chosen material model consists in a rotating damage model of the type described in Crisfield [1997] that includes effects of damage both due to tension and due to compression. The two damage effects are modelled as independent phenomena, which will be controlled by two single parameters $\alpha_t \in [0,1]$ and $\alpha_c \in [0,1]$, which represent the amount of damage undergone in the two different modes, respectively. These variables take on values which starting from 0 (no damage) increase monotonically up to 1, point at which the material has lost all its load bearing capacity. Computation of the stresses occurs always along the principal strain directions, so that the material undergoes equal degradation in all directions. To start with, the largest and smallest of the principal strains are determined as follows:

$$\varepsilon_{max} = \max(\varepsilon_1, \varepsilon_2) \tag{9}$$

$$\varepsilon_{min} = -\min(\varepsilon_1, \varepsilon_2) \tag{10}$$

where ε_1 and ε_2 are the principal strains.

Tension damage

If ε_{max} is larger than zero then there is at least one direction in which the material is in tension. A critical (variable) strain, $\varepsilon_{t,cr}$, beyond which the material deteriorates is defined as:

$$\varepsilon_{t,cr} = (\varepsilon_{t,u} - \varepsilon_t)\alpha_t + \varepsilon_t \tag{11}$$

where $\varepsilon_{t,u}$ is the ultimate crack strain, and ε_t is the strain corresponding to the tensile strength of the material, f_t, see Figure 2a. The material damage parameter is updated according to the magnitude of $\varepsilon_{t,cr}$ with respect to ε_{max}:

$$\alpha_t = \begin{cases} \alpha_t \ (\text{unchanged}) & \varepsilon_{max} \le \varepsilon_{t,cr} \\ \dfrac{\varepsilon_{max} - \varepsilon_t}{\varepsilon_{t,u} - \varepsilon_t} & \varepsilon_{t,cr} < \varepsilon_{max} < \varepsilon_{t,u} \\ 1 & \varepsilon_{t,u} \le \varepsilon_{max} \end{cases} \tag{12}$$

Finally, a stiffness reduction factor, d_t, is introduced:

$$d_t = \frac{\varepsilon_t(1-\alpha_t)}{\varepsilon'_{t,cr}} \tag{13}$$

where $\varepsilon'_{t,cr}$ is the updated value of the critical strain calculated using equation 11 and the updated value of α_t. The adjusted response of the material, which is always along a secant loading/unloading branch as shown in Figure 2, is obtained by multiplying , d_t, with Young' modulus and the appropriate principal strain.

Compression damage

Compression damage is treated in an almost identical manner except an extra feature. The initial elastic branch is followed by a flat branch where the strength of the material remains unaltered up to a strain $\varepsilon_{c,max}$. Just as in the tension model the critical strain and the updated value of α_c are obtained using formulas identical to those in 12 and 13 simply replacing the subscript's 't' with 'c'. The only change is in the stiffness reduction factor which now is given by:

$$d_c = \begin{cases} \dfrac{\varepsilon_c(1-\alpha_c)}{\varepsilon'_{c,cr}} & \varepsilon_{min} \le \varepsilon_{c,max} \\ \dfrac{\varepsilon_c}{\varepsilon'_{c,cr}}\left[1-\dfrac{\varepsilon'_{c,cr}-\varepsilon_{c,max}}{\varepsilon_{c,u}-\varepsilon_{c,max}}\right] & \varepsilon_{c,max} < \varepsilon_{min} < \varepsilon_{c,u} \\ 0 & \varepsilon_{c,u} \le \varepsilon_{min} \end{cases} \tag{14}$$

where $\varepsilon_{c,max}$ marks the end of the flat part of the stress-strain diagram; E_2 is the stiffness of the material at the secondary branch; and $\varepsilon'_{t,cr}$ refers to the updated value of $\varepsilon_{t,cr}$. Having calculated the values of the stiffness reduction factors in tension and compression, the principal stresses, $\boldsymbol{\sigma}$, can be calculated using the following equation:

$$\boldsymbol{\sigma} = E\left\{d_c\begin{bmatrix}\min(\varepsilon_1,0)\\ \min(\varepsilon_2,0)\end{bmatrix} + d_t\begin{bmatrix}\max(\varepsilon_1,0)\\ \max(\varepsilon_2,0)\end{bmatrix}\right\} \tag{15}$$

where E is Young's modulus.

Relationship with fracture energy

The values of the strains defining the various points of the stress-strain diagrams in tension and compression should be chosen in relation to the fracture energy of the material in these two modes. To do this, the area under the curves should be equal to the fracture energy divided by a length scale parameter, h, which represents a typical length of the element (e.g. the square root of the average area of the elements or the average area represented by the Gauss points in an element).

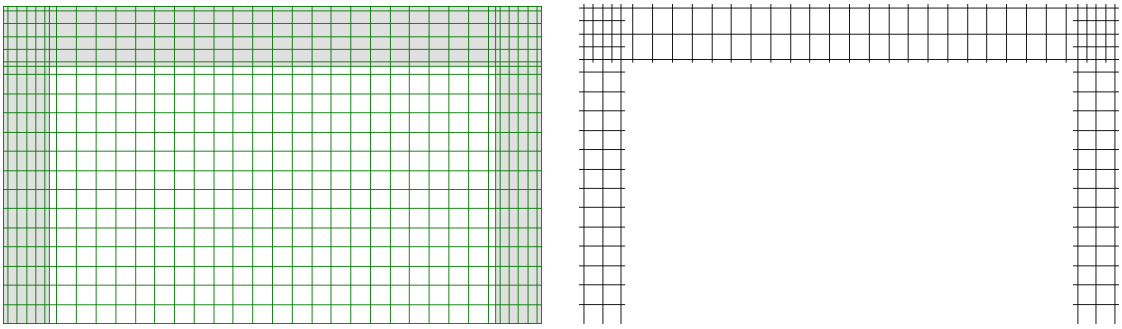

Figure 3. Infilled frame mesh and frame reinforcement.

ANALYSIS OF AN INFILLED REINFORCED CONCRETE FRAME

Description of the model

The FE mesh consists of 720 8-noded quadrilateral plane stress elements forming the r.c. frame and masonry wall and 1113 truss elements forming the reinforcement as shown in Figure 3. The steel reinforcement is modelled using 2 noded truss elements and an ideal elasto-plastic material model. The external dimensions of the frame are 3.18 m by 5.22 m, with columns of 0.45x0.45 m^2 and a beam cross section of 0.3 m by 0.6 m, and a wall thickness of 0.3m. For the concrete: E=30000 MPa, f_t=2.65 MPa, G_t=100 J/m^2, f_c=24 MPa, G_c=10000 J/m^2; and for the masonry: E=1000 MPa, f_t=0.1 MPa, G_t=20 J/m^2, f_c=2 MPa, G_c=5000 J/m^2, where G_t and G_c are the fracture energies in tension and compression respectively. Further, for the sake of simplicity, the masonry wall and r.c. frame have been modelled as though they where perfectly bonded. The load has been specified in the form of an imposed displacement of the top nodes of the two r.c. columns forming the frame. The displacement is imposed at a rate of 0.1 m/s from left to right, with the static response being determined at 1 mm intervals, using the procedure described previously. The selected time step for the analysis is 5μs, and the analysis has been carried out for two cases: the frame alone and the frame with the infill.

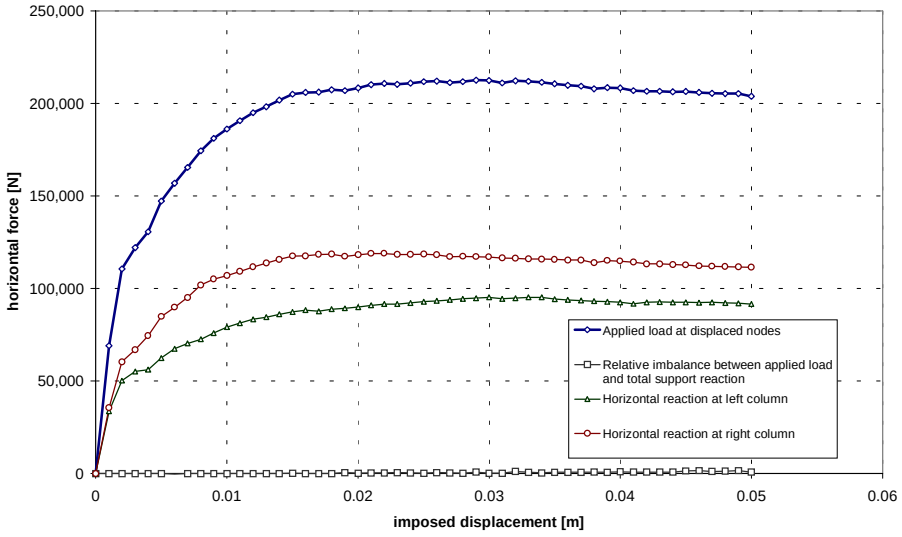

Figure 4. Response at top (displacement controlled) nodes, and horizontal support reactions (bare frame).

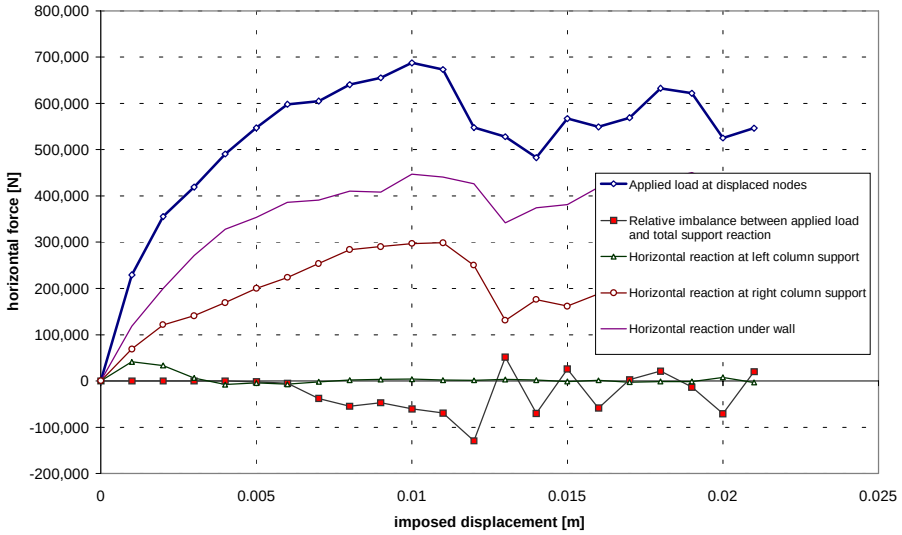

Figure 5. Response at top (displacement controlled) nodes, and horizontal support reactions for the infilled frame. Note line showing the imbalance between applied load and support reaction: beyond 5 mm displacements the accuracy of the static solution has deteriorated quite drastically.

Results

Figures 4 and 5 show the response of the bare frame and infilled frame respectively. In the bare frame an average horizontal load of about 100 kN is transferred by each column. Given the fact that the left column is in tension and therefore less stiff to bending moments, it follows that it carries slightly less load than the right column. In the infilled frame case the situation changes drastically: the total load carrying capacity has increased by about 3 times, with the wall carrying a substantial part of the horizontal load. The left column seems to have no part in transferring any of the horizontal load, whereas the load at the base of the right column has increased by 3 times. The formation of a diagonal strut mechanism is quite evident from the formation of the two large diagonal cracks in the wall. This mechanism introduces a large diagonal force in the left corner, which is counterbalanced horizontally, by the applied load, and vertically by tension in the left column. The tension in the left column is about 6 times that in the bare case frame (see Figure 7), and its presence is evident from the series of horizontal cracks that develop throughout its length.

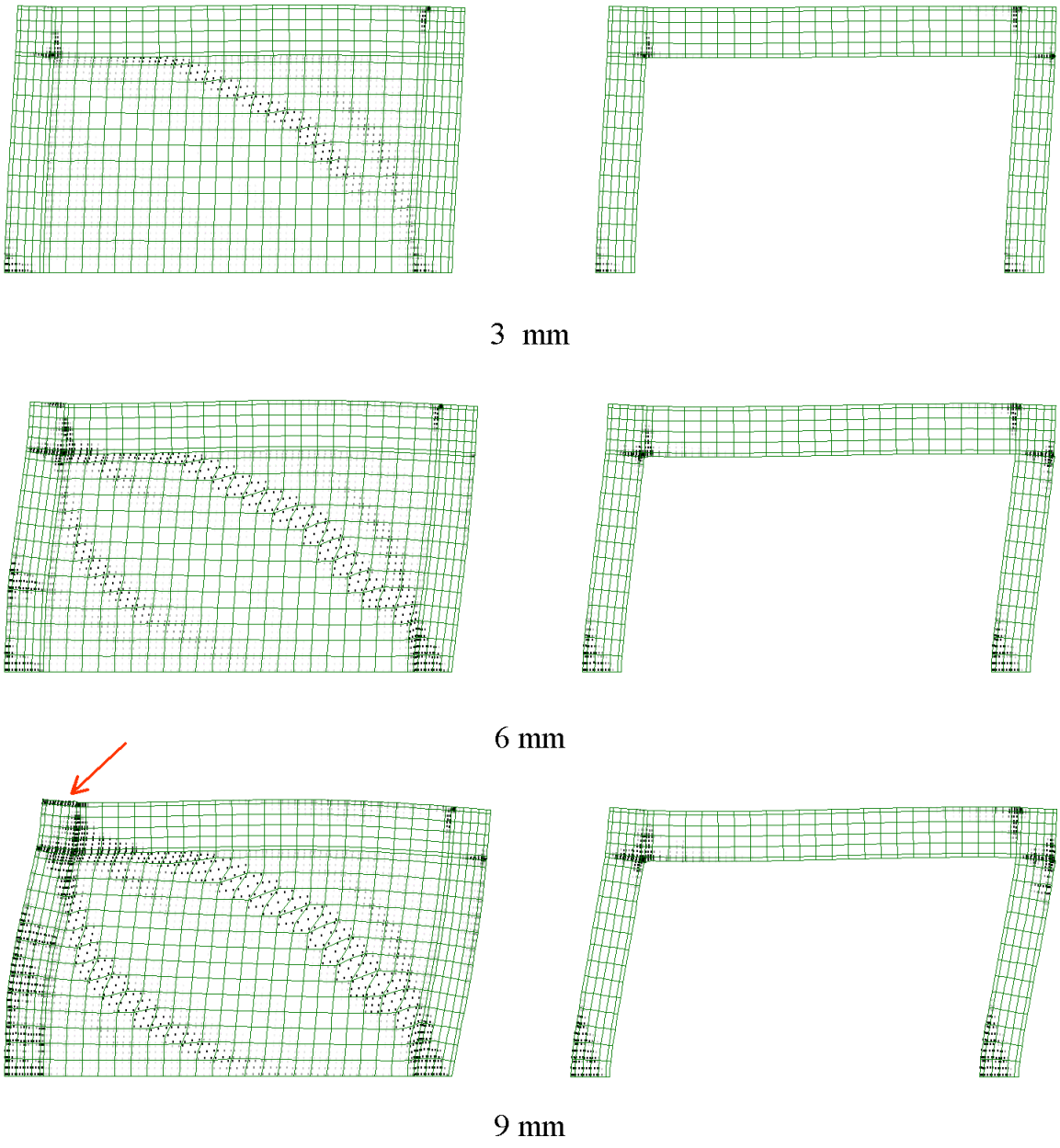

Figure 6. Deformations (50x) and material degradation in tension at 3 different displacement levels for the infilled frame and the bare frame. The degradation of the material is shown using relatively light grey or dark spots at the integration points according to the value of α_t at these points (white: α_t =0; black: α_t =1).

As a final remark, it should be mentioned that beyond 5 mm displacement there is a large inaccuracy in the equilibrium of the infilled frame (see the curve showing the imbalance in applied load and support reaction in Figure 5). This is probably due to the fact that a large horizontal crack has developed at the concrete surface where the load at the left column is being applied. The material along this zone, which is free to detach itself from the rest of the structure, introduces a certain degree of static indeterminacy making it difficult for the algorithm to find an equilibrium point (see the arrow indicating this zone of damage in the bottom left picture of Figure 6).

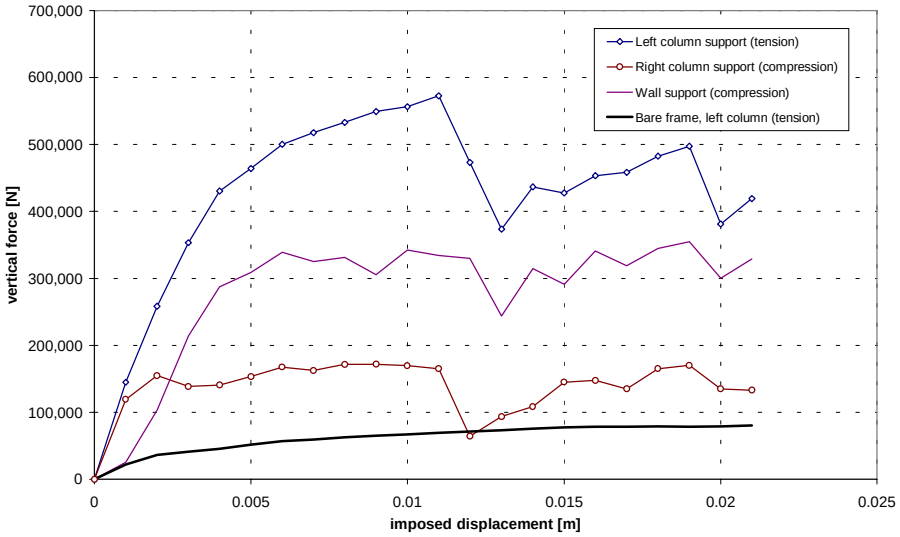

Figure 7. Comparison of vertical support reactions at the columns for the infilled frame. Note the large difference in tension in the left column between the bare frame case and the infilled frame case.

CONCLUSIONS

A procedure to determine the dynamic response of a non-linear structural problem, and a scheme that allows for the determination of the would-be static response of the structure at a specific moment in time have been presented. These methods have been applied to the problem of an infilled r.c. frame without encountering the difficulties related to material, and hence, numerical instabilities, which typically hamper finite element calculations. Although at a relatively early stage of development, these methods have led to results with a relatively reduced programming effort and will allow for a shift of focus on aspects of material and structural response.

REFERENCES:

Crisfield, M.A. (1997), *Non-linear Finite Element Analysis of Solids and Structures: Advanced Topics*, Vol. 2, Wiley, Chichester.

Galanti, F.M.B., Scarpas, A., Vrouwenvelder, A.C.W.M. (1998a), "Calibration of a numerical model for the simulation of masonry under earthquake loading", *Structures under Shock and Impact V*, Thessaloniki, June 1998, pp. 395-405. Computational Mechanics Publications, Southampton.

Galanti, F.M.B., Scarpas, A., Vrouwenvelder, A.C.W.M. (1998b), "Calibration of a capacity design procedure for infilled reinforced concrete frames", Proceedings of the 11th European Conference on Earthquake Engineering, Paris, September 1998. Balkema, Rotterdam.

Galanti, F.M.B., Scarpas, A., Vrouwenvelder, A.C.W.M., "An iterative solution scheme for non linear dynamic problems", *Submitted for publication in: Earthquake Engineering and Structural Dynamics.*